ON SIMILARITY IN THE ATMOSPHERIC BOUNDARY LAYER

ZBIGNIEW SORBJAN

Department of Atmospheric Sciences, University of Washington, Seattle, Washington, U.S.A.[1]

(Received in final form 12 August, 1985)

Abstract. A similarity theory for the atmospheric boundary layer is presented. The Monin–Obukhov similarity theory for the surface layer is a particular case of this new theory, for the case of $z \to 0$. Universal functions which are in agreement with empirical data are obtained for the stable and convective regimes.

1. Introduction

In 1954, Monin and Obukhov published their milestone paper on the similarity theory of the surface layer. The theory has proved to be one of the most successful tools in the analysis of the mean flow in the atmospheric boundary layer (ABL). The idea of similarity has provided a simple framework for determining semi-empirical distributions of the meteorological parameters in the lower atmosphere. The application of the Monin–Obukhov (M–O) theory has been limited to the lowest 10–100 m above the ground. An equally simple method to describe the flow above the surface layer has not been developed during the last three decades, mostly due to the absence of sufficient experimental data.

Since the early 1950's, however, there have been numerous experimental studies which have provided a substantial increase of our knowledge of the atmospheric boundary layer (The Great Plains 1953 Turbulence Field Program, the Wangara 1967 Experiment, Kansas 1968 Field Program, Minnesota 1973 Experiment). An extensive empirical base provided by these field experiments has been supplemented by three-dimensional numerical simulations pioneered by Deardorff and by second-order closure modeling. Employment of these contributions has made it possible to generalize M–O similarity theory to the region above the surface layer.

Our paper is divided into three parts. In the first we derive similarity profiles for the stable-continuous boundary layer, which according to Deardorff (1978) is limited by the condition $0 < h/L < 2$. In the second part we discuss the convective case, which occurs in the atmosphere, when $-z_i/L > 2$ (h, z_i – heights of the stable and convective ABL, L – Monin–Obukhov length). In the last part, we present the empirical verification of the new theory.

[1] On leave from Institute of Environmental Engineering, Warsaw Technical University, 00653 Warsaw, Poland. Present address, Department of Geological and Geophysical Sciences, University of Wisconsin, Milwaukee, WI 53201 U.S.A.

Boundary-Layer Meteorology **34** (1986) 377–397.

2. Stable Boundary Layer

Let us first discuss the case, when air is slightly warmer than the underlying surface and the turbulence is continuous in the entire boundary layer. Over land at night, this can exist only during strong winds.

In the stable atmospheric boundary layer, buoyancy suppresses turbulent eddies, which become small and independent of the distance from the surface. To express the local character of turbulence, we adopt the first hypothesis: 'The appropriate scales of turbulent flow in the stable-continuous regime are based on the local values of the Reynolds stress $\tau(z)$ and the turbulent heat flux $\overline{w'\theta'}(z)$.' We shall use:

$$\begin{aligned} &\text{velocity scale:} && U_*(z) = \tau^{1/2} \quad \text{(local friction velocity)} \\ &\text{temperature scale:} && t_*(z) = -\frac{\overline{w'\theta'}}{\tau^{1/2}} \\ &\text{height scale:} && \Lambda(z) = \frac{\tau}{\kappa\beta t_*} \quad \text{(local M–O length)} \end{aligned} \tag{1}$$

where κ – von Karman constant (= 0.35), β – buoyancy parameter. In the surface layer, (1) takes the form of M–O similarity scales u_*, T_* and L. The idea of local scaling for the stable ABL was first introduced by Nieuwstadt (1984).

We shall consider the following similarity functions:

$$\begin{aligned} &\Phi'_M = \frac{\kappa\Lambda}{U_*}\{(\partial U/\partial z)^2 + (\partial V/\partial z)^2\}^{1/2} \equiv \kappa\Lambda S/U_*; \quad \phi'_h = \frac{\kappa\Lambda}{t_*}\frac{\partial\theta}{\theta z}; \\ &\Phi_{12} = \frac{\overline{u'v'}}{U_*^2}; \quad \Phi_1 = \frac{\overline{u'^2} + \overline{v'^2}}{U_*^2} \equiv \frac{\sigma^2}{U_*^2}; \quad \Phi_w = \frac{\overline{w'^2}}{U_*^2}; \\ &\Phi_\theta = \frac{\overline{\theta'^2}}{t_*^2}; \quad \Phi_{1\theta} = \frac{\{(\overline{u'\theta'})^2 + (\overline{v'\theta'})^2\}^{1/2}}{t_* U_*} \equiv \frac{r}{t_* U_*}; \\ &\Phi_E = \frac{E}{U_*^2}; \quad \Phi'_\varepsilon = \frac{\kappa\Lambda\varepsilon}{U_*^3}, \end{aligned} \tag{2}$$

where $E = (\overline{u'^2} + \overline{v'^2} + \overline{w'^2})/2)$ – the turbulent energy; ε – the dissipation rate; S – the magnitude of the wind shear; σ – the horizontal turbulent energy; r – the horizontal heat flux; U, V, θ – the components of the wind velocity and the potential temperature. The similarity functions (2) are defined in a way analogous to the M–O similarity functions.

In the stable ABL, turbulence is in a so-called 'z-less' state (Wyngaard, 1973). As a consequence, all similarity functions in (2) should approach constant values

$$\Phi'_M, \Phi'_h, \Phi'_\varepsilon, \Phi_{1\theta}, \Phi_1, \Phi_w, \Phi_\theta, \Phi_E, \Phi_{12} \sim \text{constant}. \tag{3}$$

It is convenient to rescale the three Φ' functions, defining the following new functions:

$$\Phi_M = Z\Phi'_M; \quad \Phi_h = Z\Phi'_h; \quad \Phi_\varepsilon = Z\Phi'_\varepsilon. \tag{4}$$

Values of the universal constant in (3) can be obtained by matching the stable outer and stable surface layers. This leads to the second hypothesis: 'The form of the similarity functions Φ of $Z = z/\Lambda$ in the outer layer (the part of the ABL above the surface layer) is identical to the form of M–O similarity functions ϕ of $\zeta = z/L$ in the surface layer (L – Monin–Obukhov length)'. This is the main result of the similarity theory in the stable case.

The empirical basis of the M–O similarity theory of the surface layer gives the values of the constants in (3) and (4) (Takeuchi, 1961; Businger *et al.*, 1971; Wyngaard *et al.*, 1971; Wyngaard, 1975):

$$\begin{aligned} &\Phi_M = 1 + 4.7Z; \quad \Phi_h = 0.74 + 4.7Z; \quad \Phi_\varepsilon = 1 + 3.7Z; \\ &\Phi_1 = 8.5; \quad \Phi_w = 2.5; \quad \Phi_\theta = 4; \Phi_{1\theta} = 4. \end{aligned} \tag{5}$$

Let us notice that (5) holds in neutral stratification, for which $Z \to 0$. Functions ϕ_E, ϕ_w and ϕ_θ were previously shown to be constant by Nieuwstadt (1984).

From the definitions of eddy viscosities and Richardson numbers, we also obtain:

$$K_M = Z/\Phi_M; \quad K_H = Z/\Phi_h: \quad \mathrm{Ri} = Z\Phi_h/\Phi_M^2; \quad R_f = Z/\Phi_M \tag{6}$$

where K_M, K_H are momentum and heat eddy viscosities (nondimensionalized by $\kappa\Lambda U_*$), and Ri, R_f are Richardson numbers.

Now we introduce the third hypothesis, concerning the distribution of the Reynolds stress and the turbulent heat flux in the stable boundary layer. We assume that in the stable, barotropic ABL, over a horizontal terrain:

$$\begin{aligned} &\tau = u_*^2 (1 - z/h)^{\alpha_1} \\ &\overline{w'\theta'} = \overline{(w'\theta')}_0 (1 - z/h)^{\alpha_2} \end{aligned} \tag{7}$$

where h is the height of ABL and α_1, α_2 are constants (dependent on the state of temporal development of the stable ABL, the terrain slope, baroclinicity, etc.). Constants α_1 and α_2 must be determined empirically.

Data presented by Yokoyama *et al.* (1979) show that α_2 can vary between 1 and 3. The Minnesota observations (Caughey *et al.*, 1979), taken near sunset, show that $\alpha_1 \sim 2$ and $\alpha_2 \sim 3$ (see Figure 4). The Cabauw data (Nieuwstadt, 1984), collected later in the development of the stable ABL, indicate that both α_1 and α_2 are close to 1.

It can be shown that $\alpha_2 \geq \alpha_1$. This result can be obtained from (2), (4), (5), (7), and from the assumption that both S and $\partial\theta/\partial z \to 0$ when $z/h \to 1$. The vanishing of the gradients at the top of the ABL simply means that the stable regime develops by cooling of the daytime mixed layer and that at $z = h$, the wind velocity reaches a maximum. The condition of $\alpha_1 \geq \alpha_2$ was not met in Nieuwstadt's (1984) study. This caused his results to exhibit a singularity in the temperature profile at the top of the ABL.

From (7) we obtain:

$$U_* = u_*(1 - z/h)^{\alpha_1/2}$$
$$t_* = T_*(1 - z/h)^{\alpha_2 - \alpha_1/2} \tag{8}$$
$$\Lambda = L(1 - z/h)^{3/2\alpha_1 - \alpha_2}$$

where L – Monin–Obukhov length, ($L = u_*^2/(\kappa\beta T_*)$ and $(\overline{w\theta})_0 = -u_* T_*$).

For the particular case of the Minnesota experiment (Caughey *et al.*, 1979) when $\alpha_1 = 2$ and $\alpha_2 = 3$, from (5), (6), and (8) we obtain

$$\frac{\kappa z}{u_*} S = (1 + 4.7\mu_h z/h)(1 - z/h) \tag{9}$$

$$\frac{\kappa z}{T_*} \frac{\partial\theta}{\partial z} = (0.74 + 4.7\mu_h z/h)(1 - z/h)^2 \tag{10}$$

$$\frac{\sigma^2}{u_*^2} = 8.5(1 - z/h)^2 \tag{11}$$

$$\frac{\overline{w'^2}}{u_*^2} = 2.5(1 - z/h)^2 \tag{12}$$

$$\frac{\overline{\theta'^2}}{T_*^2} = 4(1 - z/h)^4 \tag{13}$$

$$\frac{\kappa h\varepsilon}{u_*^3} = (1 + 3.7\mu_h z/h)\frac{(1 - z/h)^3}{z/h} \tag{14}$$

$$\frac{r}{u_* T_*} = 4(1 - z/h)^3 \tag{15}$$

$$\mathrm{Ri} = \mu_h \frac{z/h}{(1 + 4.7\mu_h z/h)^2}(0.74 + 4.7\mu_h z/h) \tag{16}$$

$$R_f = \mu_h \frac{z/h}{1 + 4.7\mu_h z/h} \tag{17}$$

$$\frac{k_M}{\kappa u_* h} = \frac{z/h(1 - z/h)}{1 + 4.7\mu_h z/h} \tag{18}$$

$$\frac{k_H}{\kappa u_* h} = \frac{z/h(1 - z/h)}{0.74 + 4.7\mu_h z/h} \tag{19}$$

where $\mu_h = h/L$ – the stability parameter. The integration of (10) gives the temperature

profile:

$$\kappa \frac{\theta(z) - \theta(0)}{T_*} = 0.74\{\ln(z/z_0) - 2z/h + 0.5(z/h)^2 + \\ + 4.7\mu_h z/h[1 - z/h + 1/3(z/h)^2]\} \tag{20}$$

where z_0 is the roughness parameter.

Let us emphasize that the power coefficients in (9)–(20) are not universal, and were found for the case of the evolving boundary layer during the Minnesota experiment.

The comparison of the above functions with observations will be given in Section 4, here we only notice that when $z/h \to 0$, all functions (9)–(19) take the classic form of the semi-empirical surface-layer similarity functions.

3. Convective Boundary Layer

Let us now consider the case of a large upward heat flux and light winds, when the structure of the ABL is completely dominated by buoyancy (so-called free convection regime). The upper part of the daytime ABL over land is almost always convective.

In free convection, the product of the Reynolds stress with wind shear is relatively small so the stress cannot be used to define local scales. This remark leads to the hypothesis: 'The appropriate scales of turbulent flow in the convective regime, below the entrainment layer, are based on the local values of the turbulent heat flux $\overline{w'\theta'}(z)$.' We shall use:

$$\text{velocity scale: } u_f(z) = [\beta z \overline{w'\theta'}]^{1/3}$$

$$\text{temperature scale: } t_f(z) = -\frac{\overline{w'\theta'}}{u_f} = -\left[\frac{(\overline{w'\theta'})^2}{\beta z}\right]^{1/3} \tag{21}$$

$$\text{height scale: } -\frac{u_f^2}{\beta t_f} \equiv z\,.$$

The above hypothesis is in accord with the general argument of Tennekes and Lumley (1972), that if the turbulence time scales are small enough to permit adjustment to the gradually changing environment, it is possible to assume that the turbulence is dynamically similar, if nondimensionalized by local scales. In our case, the time scale of the energy-containing turbulent eddies is $\tau_t \sim z_i/w_* \sim 10$ min (z_i – the height of ABL and w_* the velocity scale, defined by Equation (28) and is small in comparison with diurnal cycle and time changes in the synoptic conditions.

The actual height z in (21) is a proper scale of height in the lower half of the convective ABL as a result of mechanical dumping of energetic long-wave fluctuations due to the presence of a solid lower boundary.

In the convective surface layer, where $\overline{w'\theta'}$ = const, (21) take the form of the free convection scales u_{f0}, t_{f0} (Wyngaard *et al.*, 1971; Wyngaard, 1973). We consider the

following similarity functions:

$$\Phi_M = \frac{\kappa z}{u_f} S, \quad \Phi_h = \frac{\kappa z}{t_f} \frac{\partial \theta}{\partial z}, \quad \Phi_w = \frac{\overline{w'^2}}{u_f^2}, \quad \Phi_\theta = \frac{\overline{\theta'^2}}{t_f^2}$$

$$\Phi_{1\theta} = \frac{\overline{u'\theta'}}{u_f t_f}, \quad \Phi_{3\theta} = \frac{\overline{w'\theta'^2}}{u_f t_f^2}, \quad \Phi_{w3} = \frac{\overline{w'^3}}{u_f^3}. \tag{22}$$

From (21) it follows that z is the only height scale and therefore it is impossible to construct the dimensionless height parameter in the convective ABL. As a consequence, all universal functions obeying local similarity must be constant:

$$\Phi_h, \Phi_w, \Phi_\theta, \Phi_{1\theta}, \Phi_{3\theta}, \Phi_{w3} \sim \text{constant}. \tag{23}$$

The same argument was used to determine the form of the similarity functions in the convective surface layer (Wyngaard, 1973).

Not all statistics obey local similarity. The dissipation rate of the turbulent energy and the horizontal wind variances are approximately constant in the mixed layer (Caughey and Palmer, 1979) and therefore cannot remain constant when scaled by (21). The velocity spectra for the horizontal wind components show a weak dependence on height (Kaimal *et al.*, 1976), confirming that (21) are not appropriate scales for these statistics. In contrast, the spectrum of the third velocity component, w, has a very distinct spread with height, justifying the use of z as a height scale up to $z/z_i \sim 0.5$. Also in the spectrum of temperature there is a strong dependence on height (Kaimal *et al.*, 1976), indicating that Φ_θ follows local similarity. The functions Φ_w and Φ_θ were empirically shown to be constant by Caughey and Readings (1974, 1975), who found $\Phi_w = 1.21$ and $\Phi_\theta = 1.85$.

Now, as was done for the stable boundary layer, we assume the form of the turbulent heat flux (Lilly, 1968):

$$\overline{w'\theta'} = (\overline{w'\theta'})_0 [(1 - z/z_i)^{\alpha_1'} - \alpha_2' z/z_i] \tag{24}$$

where z_i is the height of the convective ABL, α_1' is a constant and α_2' parameterizes entrainment at the top of the ABL. Also in this case the choice of constants is debatable; however, there is general agreement that $\alpha_1' = 1$ and $\alpha_2' = 0 \div 1$.

From this we have

$$\overline{w'\theta'} = (\overline{w'\theta'})_0 (1 - \alpha z/z_i) \tag{25}$$

where $\alpha = 1 + \alpha_2'$,
and also

$$u_f = u_* \left(-\frac{z}{\kappa L} \right)^{1/3} (1 - \alpha z/z_i)^{1/3} = w_* \left(\frac{z}{z_i} \right)^{1/3} (1 - \alpha z/z_i)^{1/3} \tag{26}$$

$$t_f = T_* \left(-\frac{z}{\kappa L} \right)^{-1/3} (1 - \alpha z/z_i)^{2/3} = \theta_* \left(\frac{z}{z_i} \right)^{-1/3} (1 - \alpha z/z_i)^{2/3} \tag{27}$$

where

$$u_*/w_* = (-\kappa/\mu_i)^{1/3}$$
$$T_*/\theta_* = (-\mu_i/\kappa)^{1/3} \tag{28}$$

and w_* and θ_* are the mixed-layer scales (Deardorff, 1977) and $\mu_i = z_i/L$.

Using (22), (26), and (27) we get:

$$\frac{\kappa z}{T_*}\frac{\partial\theta}{\partial z} \sim \left(-\frac{z}{L}\right)^{-1/3}(1-\alpha z/z_i)^{2/3} = \phi_h(z/L)(1-\alpha z/z_i)^{2/3}$$
$$\frac{\overline{w_2'}}{u_*^2} \sim \left(-\frac{z}{L}\right)^{2/3}(1-\alpha z/z_i)^{2/3} = \phi_w(z/L)(1-\alpha z/z_i)^{2/3}$$
$$\frac{\overline{\theta'^2}}{T_*^2} \sim \left(-\frac{z}{L}\right)^{-2/3}(1-\alpha z/z_i)^{4/3} = \phi_\theta(z/L)(1-\alpha z/z_i)^{4/3}$$
$$\frac{\overline{u'\theta'}}{u_* T_*} \sim (1-z/z_i) \tag{29}$$
$$\frac{\overline{w'\theta'^2}}{u_* T_*} \sim \left(-\frac{z}{L}\right)^{-1/3}(1-\alpha z/z_i)^{5/3} = \phi_{3\theta}(z/L)(1-\alpha z/z_i)$$
$$\frac{\overline{w'^3}}{u_*^3} \sim \left(-\frac{z}{L}\right)(1-\alpha z/z_i) = \phi_{w^3}(z/L)(1-\alpha z/z_i)$$

where $\phi(z/L)$ are semi-empirical functions in the surface layer.

Assuming that $(1/T_*\,\partial\theta/\partial z)/(1/u_*\,\partial U/\partial z)$ should remain finite, when $-z/L \to \infty$ (Monin and Obukhov, 1954), we obtain

$$\Phi_M = \frac{\kappa z}{u_f}\frac{\partial U}{\partial z} \sim (1-\alpha z/z_i)^{1/3}/(-z/L)^{2/3} \tag{30}$$

and after rescaling:

$$\frac{\kappa z}{u_*}\frac{\partial U}{\partial z} \sim (-z/L)^{-1/3}(1-\alpha z/z_i)^{2/3} = \phi_M(z/L)(1-\alpha z/z_i)^{2/3}. \tag{31}$$

It should be mentioned that the form of the free-convection surface similarity functions ϕ [in Equations (29), (31)] as well as values of the constants given by different authors differ substantially. There is a controversy, for example, connected with the form of the functions ϕ_M and ϕ_h in the surface layer. In spite of theory, which predicts a '$-1/3$' power law, Businger *et al.* (1971) obtained from the Kansas data a '$-1/2$' power behavior for ϕ_h and '$-1/4$' for ϕ_M, in the range of z/L up to -2, the largest value found. However, because of the limited z/L range and the difficulty of measuring

vanishing temperature gradients, this cannot be taken as a decisive test. There are similar difficulties with adopting other surface-layer similarity functions and their region of validity. This implies the need for more detailed observations.

Using the Minnesota 1973 data (Izumi and Caughey, 1976; Kaimal *et al.*, 1976) we found the following formulas:

$$\Phi_M = 0.42(1 - \alpha z/z_i)^{1/3}/(-\mu_i z/z_i)^{2/3} \tag{32}$$

$$\Phi_h = 0.35 \tag{33}$$

$$\Phi_{3\theta} = 1.0 \tag{34}$$

$$\Phi_w = 1.6 \tag{35}$$

$$\Phi_\theta = 2.0 \tag{36}$$

$$\Phi_{1\theta} = 0.5 \tag{37}$$

and after rescaling:

$$\frac{\kappa z_i}{w_*}\,\partial u/\partial z = 0.42(1 - \alpha z/z_i)^{2/3}/[(z/z_i)^{4/3}(-\mu_i)^{2/3}] \tag{38}$$

$$\frac{\kappa z_i}{\theta_*}\,\partial\theta/\partial z = 0.35(1 - \alpha z/z_i)^{2/3}/(z/z_i)^{4/3} \tag{39}$$

$$\frac{\overline{w'\theta'^2}}{w_*\theta_*^2} = 1.0(1 - \alpha z/z_i)^{5/3}/(-\mu_i z/z_i)^{1/3} \tag{40}$$

$$\frac{\overline{w'^2}}{w_*^2} = 1.6(z/z_i)^{2/3}(1 - \alpha z/z_i)^{2/3} \tag{41}$$

$$\frac{\overline{\theta'^2}}{\theta_*^2} = 2.0(1 - \alpha z/z_i)^{4/3}/(z/z_i)^{2/3} \tag{42}$$

$$\frac{\overline{u'\theta'}}{w_*\theta_*} = 0.5(1 - \alpha z/z_i). \tag{43}$$

Using the APTEX data (Lendschow *et.al.*, 1980) we also found

$$\Phi_{w3} = 0.8 \tag{44}$$

and

$$\frac{\overline{w'^3}}{w_*^3} = 0.8\, z/z_i(1 - \alpha z/z_i). \tag{45}$$

The application of the above formulas is limited to the lower portion of the ABL where $z/z_i < 1/\alpha$. For small values of z/z_i all functions (38)–(43) and (45) take the classic

form of the semi-empirical surface-layer similarity functions. We shall compare the obtained similarity functions with empirical data in the next section.

4. Theory Versus Observations

In the previous two sections, we developed a similarity theory of the atmospheric boundary layer. It was based on the following hypotheses:

(1) Local values of the heat flux and the Reynold stress (only in the stable and neutral cases) can be used to define characteristic scales of the motion in the atmospheric boundary layer;

(2) Similarity functions nondimensionalized by local scales have a simple form prescribed by Equations (3) and (23);

(3) The local scales of motion can be expressed as empirical functions of z/h or z/z_i.

Using hypotheses 2 and 3, we are able to express similarity functions in the form (9)–(19) and (29), (31) and extend Monin–Obukov similarity theory above the surface layer. We shall examine these hypotheses using experimental data. We shall first concentrate on the stable boundary layer.

Plots of the empirical similarity functions, nondimensionalized by local scales, were first presented by Nieuwstadt (1984). Generally, they behave like the derived formulas (5)–(6). The evidence for the functions Φ_w, Φ_θ and Ri is given in Figures 1–3. The scatter seen in these plots may be due to measurement errors, which are substantial in the stable ABL (since turbulent characteristics are small). Nevertheless, a comparison of

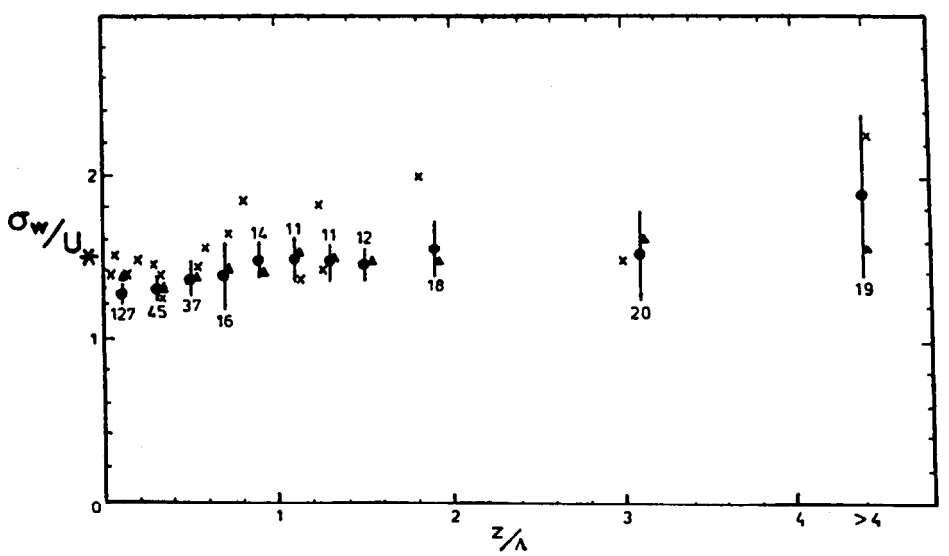

Fig. 1. Standard deviation of the vertical velocity $\sigma_w = (\overline{w'^2})^{1/2}$, nondimensionalized by a local parameter U_*, as functions of z/Λ. Stable case. Solid circles – averaged nonfiltered data, triangles – filtered data, crosses – data of Caughey *et al.* (1979) (after Nieuwstadt, 1984).

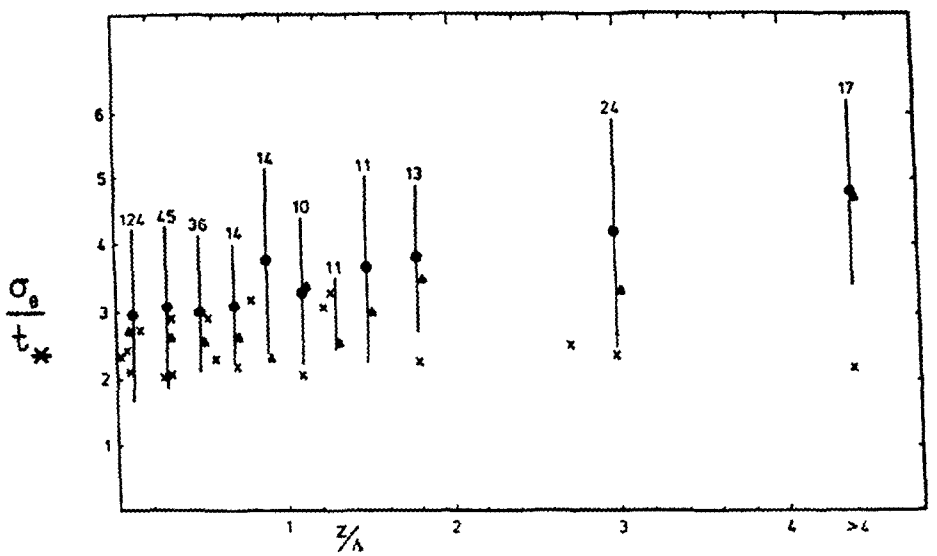

Fig. 2. Standard deviation of the temperature fluctuations $\sigma_\theta = (\overline{\theta'^2})^{1/2}$, nondimensionalized by a local parameter t_*, as functions of z/Λ. Stable case (after Nieuwstadt, 1984) (crosses are data of Caughey *et al.*, 1979).

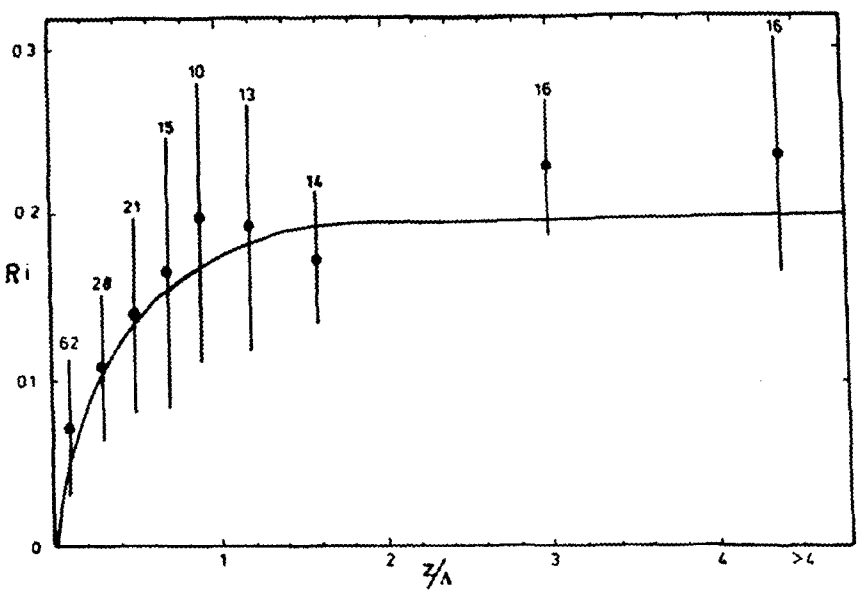

Fig. 3. Richardson number Ri as a function of z/Λ. Stable case (after Nieuwstadt, 1984). The curve is described by Equation (16).

Equations (5) and (6) with the empirical results presented by Nieuwstadt (1984) shows that hypothesis (2) is valid with respect to functions Φ_1, Φ_w, Φ_θ, Φ_E, $\Phi_{1\theta}$, K_m, K_H, Ri in the stable case. We do not possess data to examine hypotheses dealing with the

remaining functions (Φ_M, Φ_h, Φ_ε, Φ_{12}). However, we shall be able to analyze expressions (11)–(16) using the 1973 Minnesota data presented by Caughey *et al.* (1979).

Figure 4 shows the empirical distribution of the Reynolds stress and the turbulent heat flux as a function of z/h from observations in Minnesota. In the figure, Equation (8) is

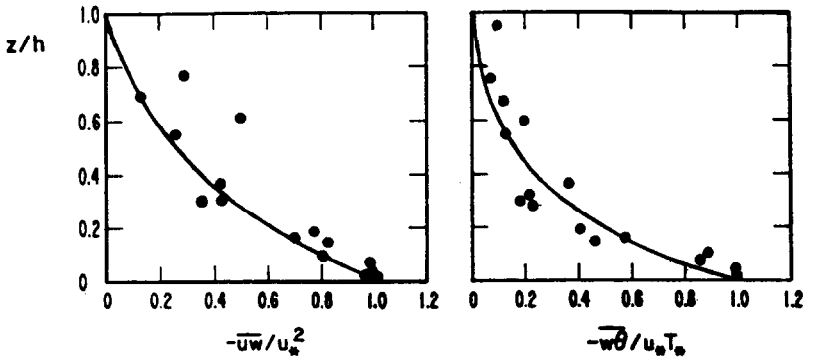

Fig. 4. Vertical profiles of the dimensionless Reynolds stress and the vertical heat flux. Stable case (after Caughey *et al.*, 1979). The curves are described by Equation (7) $\alpha_1 = 2$ and $\alpha_2 = 3$.

also plotted, fitting the data very well. In Figures 5–8, Equations (11)–(16) are plotted versus the Minnesota data. The curves fit the data remarkably well, which confirms the theory for the stable case. It should be noticed that the theory applies as well to the evolving-in-time stable ABL (Caughey *et al.*, 1979) as to the more steady state, stable ABL (Nieuwstadt, 1984).

Yamada (1979) derived vertical profiles for τ, $\overline{w'\theta'}$, $\overline{w'^2}$, $\overline{\theta'^2}$, K_M and $d|\mathbf{V}|/dZ$ for the stable case by a direct transformation of the simplified second-moment equations. Yamada's profiles have a more complicated form and are expressed in terms of the Richardson number and the momentum flux (which has the form given by Equation (7),

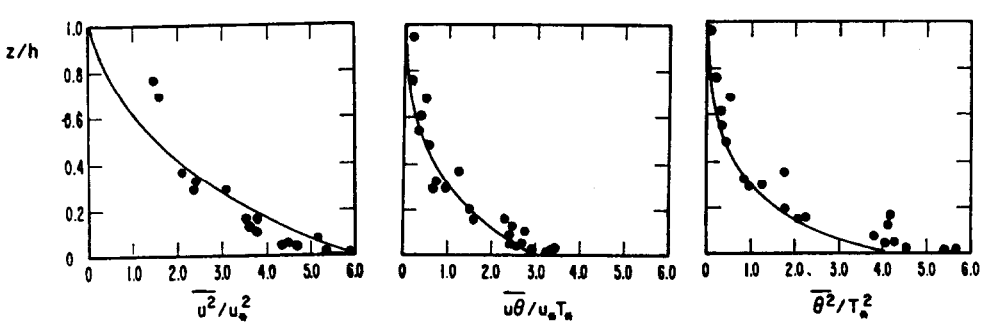

Fig. 5. Vertical profiles of the dimensionless variances and covariances. Stable case (after Caughey *et al.*, 1979). The curves are described by Equations (11), (13), (15). (Coefficients in Equations (11) and (15) are reduced to 6 and 3.)

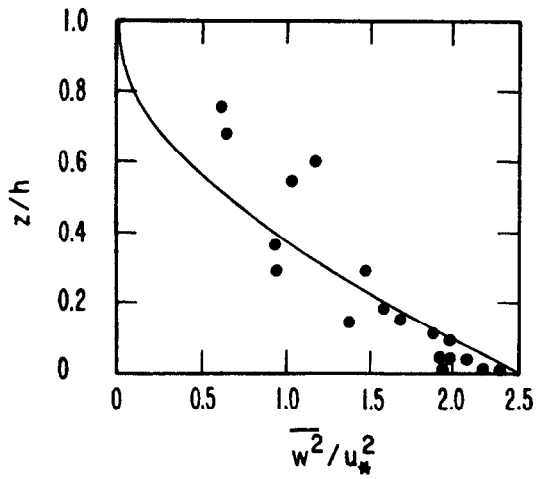

Fig. 6. Vertical velocity variance $\sigma_w^2 = \overline{w'^2}$ nondimensionalized by U_*. Stable case (after Caughey *et al.*, 1979.) The curve is described by Equation (12).

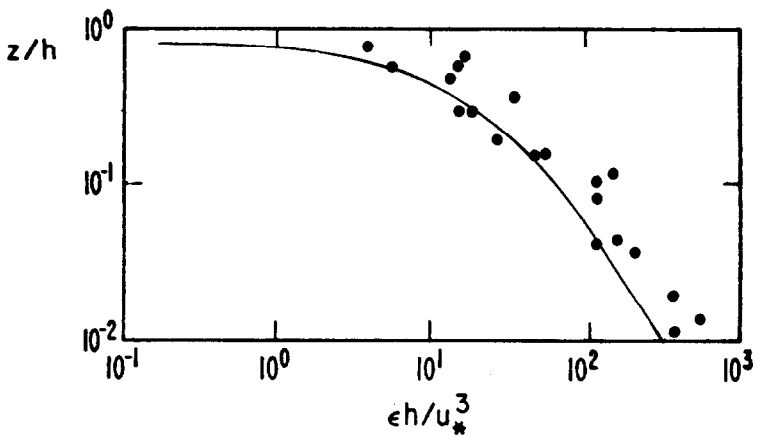

Fig. 7. Vertical profile of dimensionless dissipation rate (after Caughey *et al.*, 1979). The curve is described by Equation (14).

with $\alpha_1 = 3/2$). Eliminating the Richardson number from his formulas by the use of Equation (17) gives different but quite close expressions to those obtained in our paper.

Now we turn to the free convection case. As was done for the previous case, we shall start by examining the behavior of the similarity functions nondimensionalized with local scales. The empirical similarity functions Φ_M, Φ_h, Φ_w, Φ_θ, $\Phi_{1\theta}$ obtained from the Minnesota experiment (Izumi and Caughey, 1976) are shown in Figures 9–12. We found the functions Φ_M and Φ_h by differentiating polynomials in ln z, fitted to wind velocity and temperature measurements. Second- and third-order polynomials in ln z were used for the temperature measurements and second-order polynomials for the wind velocity.

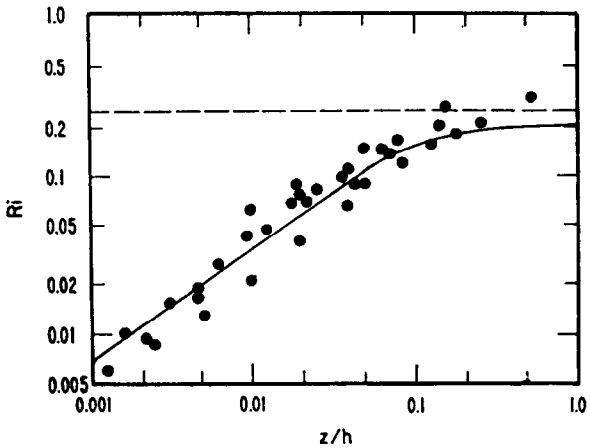

Fig. 8. Richardson number as a function of z/h (after Caughey *et al.*, 1979). The curve is described by Equation (16), $\mu_h = 5$.

The five runs with the smallest wind direction changes with height were used for this purpose. The other functions Φ were found from analysis of all 11 runs of the Minnesota experiment.

From Figures 9–12, it follows that hypotheses (23) and (30) generally work quite well. The scatter of all functions close to the top of the ABL is connected with the fact

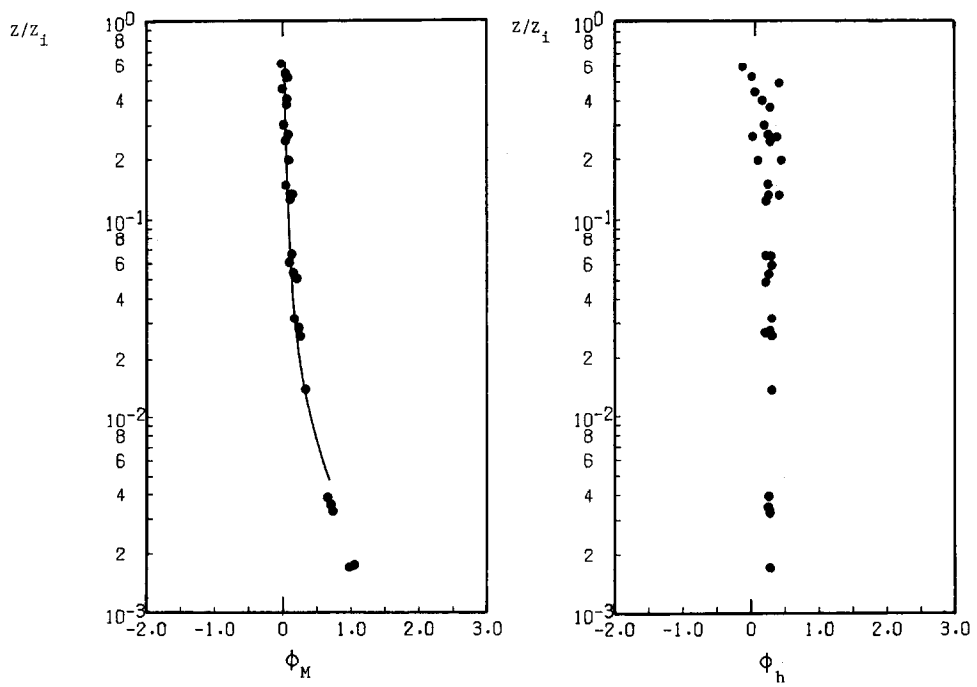

Fig. 9. Similarity functions Φ_M and Φ_h. The curve is described by Equation (32) ($\alpha = 1.5$, $\mu_i = -100$).

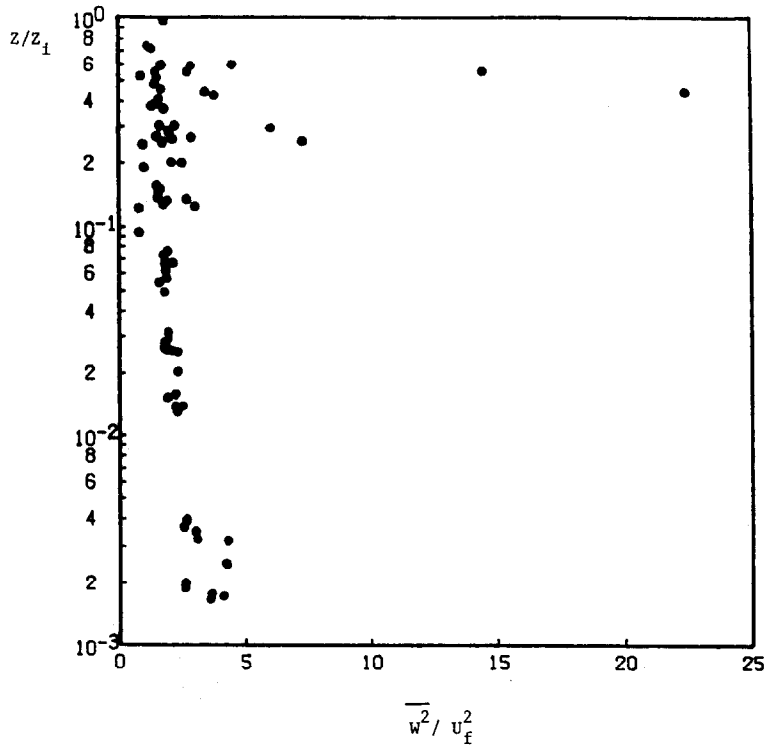

Fig. 10. Vertical velocity variance nondimensionalized by a local parameter u_f, obtained from Minnesota 1973 data (11 runs). Values of u_f decrease with height; this is responsible for scatter near the top of the ABL.

[according to (26)–(27)], that when $z/z_i \to 1/\alpha$, the scaling parameters u_f and t_f tend to zero (notice that this scatter disappears on the plots of rescaled functions in Figures 13–16). This defines the range of z where the theory is valid ($z/z_i < 1/\alpha$).

Controversy about the form of the surface similarity functions ϕ_M and ϕ_h suggests testing the following equations, obtained from Equations (38) and (39):

$$\phi_M = \frac{\kappa z}{u_*}\,\partial U/\partial z = 0.60(-z/L)^{-1/3}(1 - \alpha\mu_i^{-1} z/L)^{2/3}$$
$$\phi_h = \frac{\kappa z}{T_*}\,\partial\theta/\partial z = 0.25(-z/L)^{-1/3}(1 - \alpha\mu_i^{-1} z/L)^{2/3}. \tag{46}$$

The above functions fit the Minnesota data in Figure 13 well, for $-z/L > 0.5$, and support the free convection law '$-1/3$' in the surface layer, Constants 0.60 and 0.25 in Equations (46) can be compared with the constant 0.38, obtained by Zilitinkevich and Chalikov (1968) for ϕ_M and ϕ_h, in the range of $-0.15 < z/L < -1.2$. The region $-z/L < 0.5$ in Figure 13, where there is a discrepancy between curves and observations, can be interpreted as a transition layer to the neutral regime.

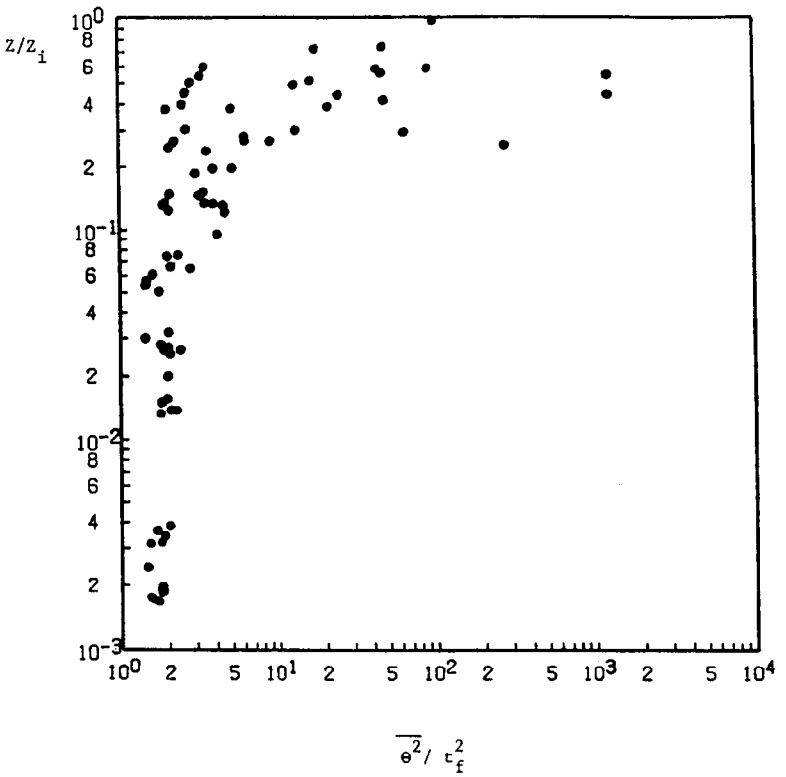

Fig. 11. Temperature variance, nondimensionalized by a convective local parameter t_f. Obtained from Minnesota 1973 data (11 runs). Values of t_f decrease with height; this is responsible for scatter near the top of the ABL.

The function ϕ_h in (46) decreases with height, reaching zero at $(z/z_i)_0 = 1/\alpha$. From this we conclude that the theory predicts a minimum in the potential temperature profile at the height where the heat flux becomes zero and therefore is unable to predict regions of the so-called 'counter-gradient flux', often observed in the mixed layer during periods of strong convection. For this reason ϕ_h is not valid near the height $(z/z_i)_0$.

Analyzing profiles of the heat flux distribution during the Minnesota experiment, we found a mean value of α about 2.2 for all runs, and equal to 1.5 for runs chosen to derive functions Φ_M and Φ_h. We also established that $\alpha \sim 1.5$ for run 7D1, $\alpha \sim 2.5$ for run 5A1 and $\alpha \sim 1.8$ as a mean for runs shown in Figure 16. All curves in Figures 13–16 represent mean conditions and are plotted for the appropriate mean values of α. The mean value $\alpha \sim 1.1$ was found for the AMTEX data (Lenschow *et al.*, 1980), shown in Figure 17.

In Figures 14 and 15 we plotted Equations (41) and (42) versus empirical data from the Minnesota experiment (two cases; 7D1 and 5A1). From these figures it follows that $\overline{\theta'^2}/\theta_*^2$ is particularly close to our prediction, given by Equation (42) in the lower half of the ABL. The region of large values of the temperature variance (not shown in the figures), near the top of the mixed layer, is excluded from our theory. Figure 16 supports

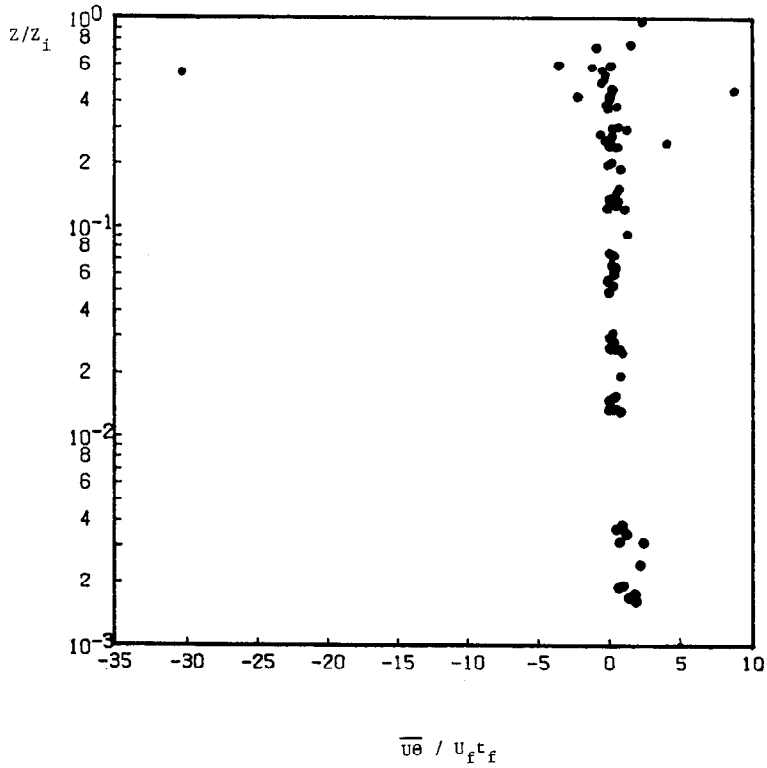

Fig. 12. Horizontal heat flux $\overline{u'\theta'}$, nondimensionalized by convective scales u_f and t_f, obtained from Minnesota 1973 data (11 runs). Values of u_f and t_f decrease with height; this is responsible for scatter near the top of the ABL.

the validity of Equation (40). In Figures 17 and 18 Equations (43) and (45) are plotted, fitting data well in the whole ABL.

These figures allow us to conclude that in the convective case our local similarity theory seems to work quite well for all considered functions. Equation (40)–(42) have for $z/z_i \to 0$ the same form (with very slightly different constants) as surface-layer formulas found by Kaimal *et al.* (1976) and Lenschow *et al.* (1980). For $z/z_i \to 1$, Equations (41) and (42) agree with formulas obtained by Yamada (1979).

The application of the theory can be depicted on the schematic sketch in Figure 19. The vertical axis on the sketch emphasizes the vertical structure of the ABL and the horizontal one shows the impact of the stability. Vertically, the ABL consists of the surface layer (with the approximately constant turbulent fluxes) up to $z/h \sim 0.1$ and the outer layer above. With respect to stability, we can classify the ABL into: convective, unstable, neutral, stable-continuous, and stable-sporadic regimes. The characteristic features of these were explained by Arya (1982). Lines inclined by the angle 45° to the left and to the right are parametric curves with h/L or z_i/L = constant. Moving along these lines changes only z. Since the absolute value of L is seldom less than 5 m, the

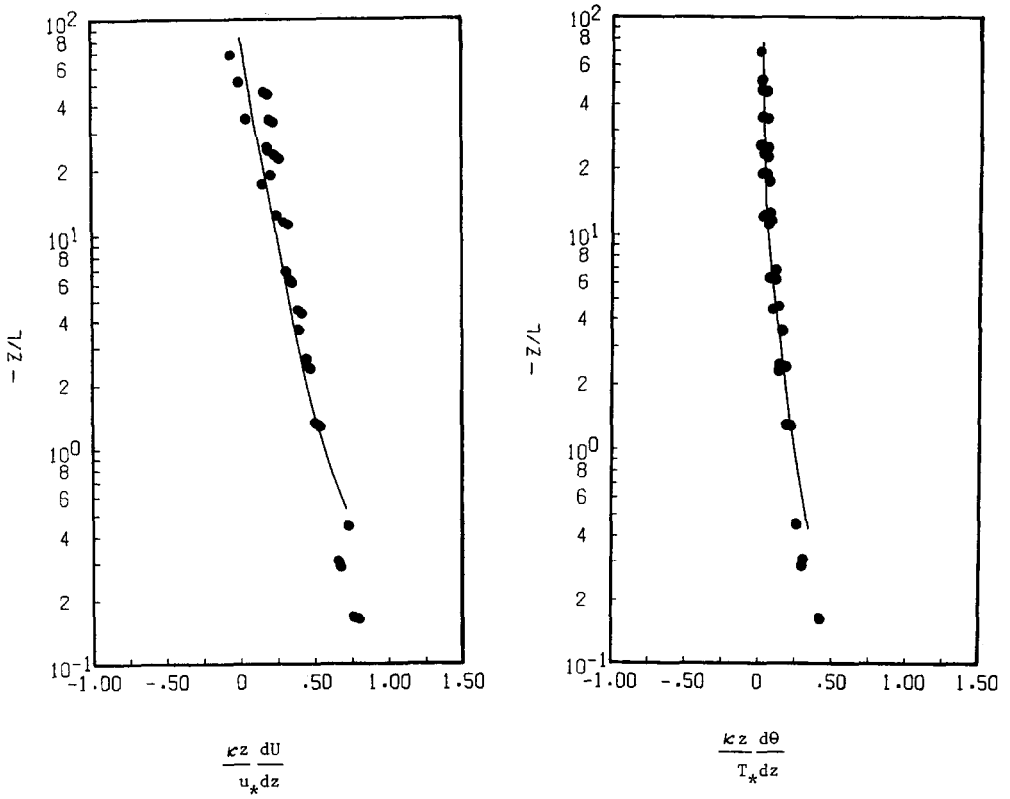

Fig. 13. Dimensionless wind and temperature gradients as functions of z/L. The curves obtained from Equation (46) for $\alpha = 1.5$ $\mu_i = -100$.

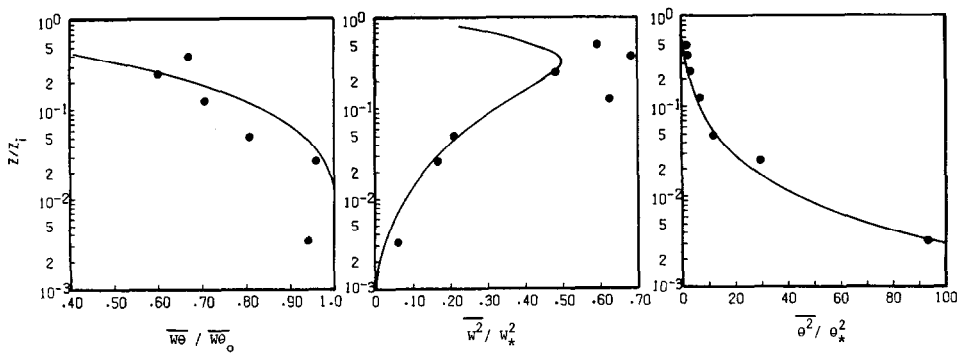

Fig. 14. Dimensionless vertical heat flux, vertical velocity variance and temperature variance. Run 7D1 from Minnesota 1973 data. The curves described by Equations (25), (41), (42); $\alpha = 1.5$.

stratification is always neutral (logarithmic sublayer) very close to the ground and turns into stable or unstable above. The free convective regime never occurs next to the ground. The upper part of the non-stable ABL is under the direct influence of entrain-

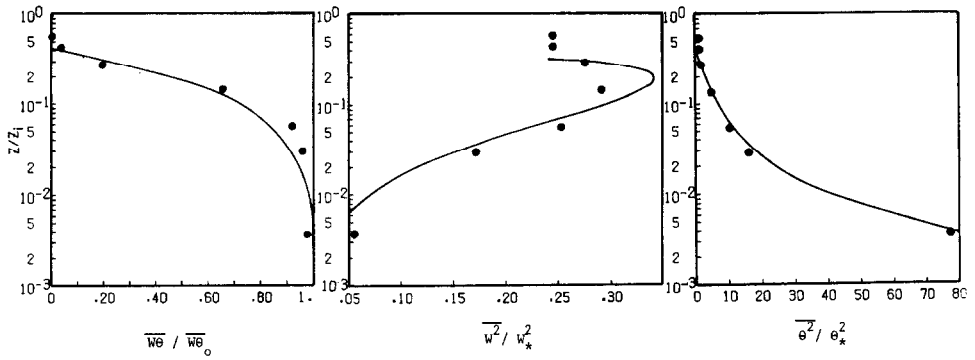

Fig. 15. Dimensionless vertical heat flux, vertical velocity variance and temperature variance. Run 5A1 from Minnesota 1973 data. The curves described by Equations (25), (41), (42); $\alpha = 2.5$.

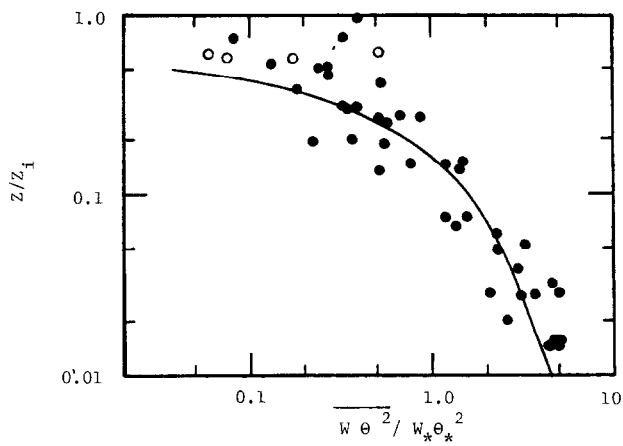

Dimensionless moment $\overline{w'\theta'^2}$. The curve described by Equation (40) (data points after Kaimal *et al.*, 1976). $\alpha = 1.8$.

ment (entrainment sublayer). The theory is not valid for the stable-sporadic regime, which needs more theoretical and empirical consideration, or near the entrainment layer. The unstable outer layer was not discussed in our paper; however, the similarity functions in this region can be obtained by matching the neutral and convective layers.

5. Conclusion

We have shown that there is a simple extension of the Monin–Obukhov similarity theory to the region above the surface layer. This has been accomplished by extending scaling parameters of the surface layer, which are u_*, T_* in the stable case and u_{f0} and θ_{f0} in the convective regime into their local (z-dependent) values.

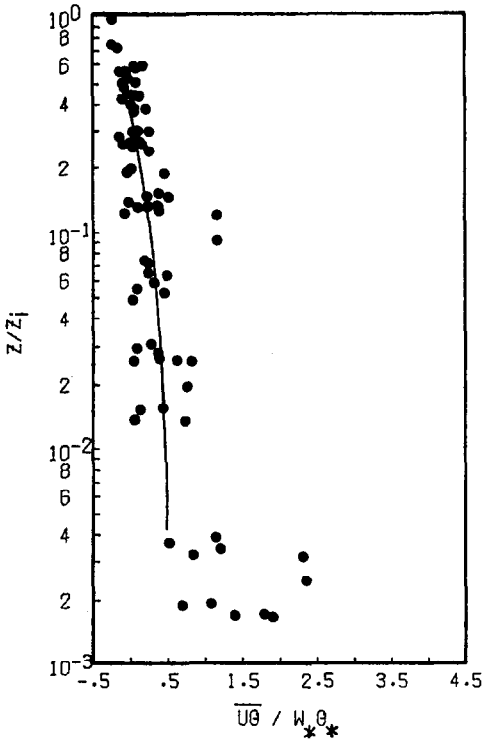

Dimensionless horizontal heat flux obtained from Minnesota 1973 data (11 runs). The curve described by Equation (43), $\alpha = 2.2$, $\mu_i = 136$.

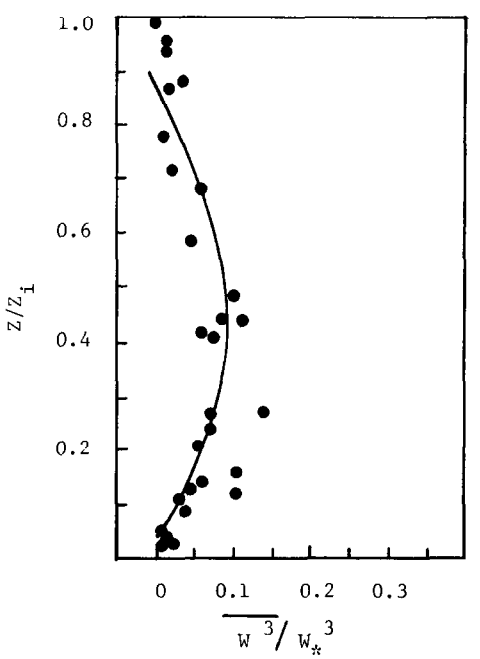

Fig. 18. Dimensionless moment $\overline{w'^3}$. The curve described by Equation (45) (data points after Lenschow *et al.*, 1980). $\alpha = 1.1$.

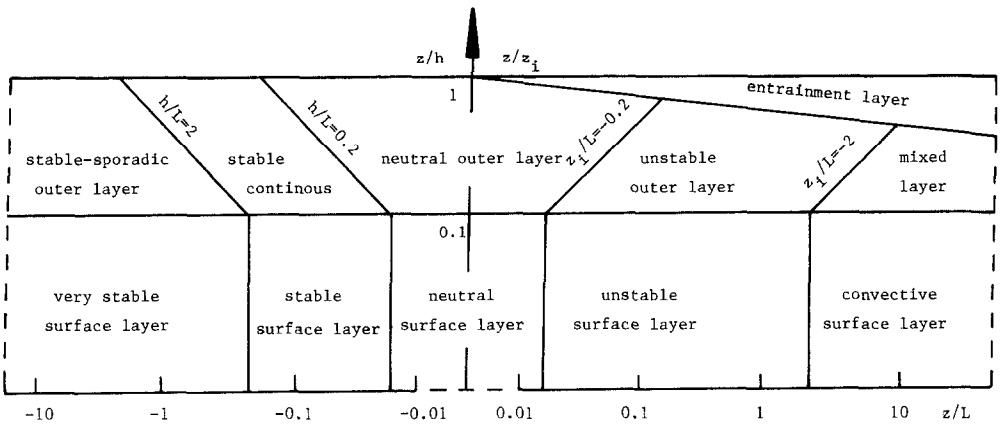

Fig. 19. Idealization of the vertical structure of the atmospheric boundary layer.

It has been found that characteristics of the flow, nondimensionalized by local parameters, have a form identical to the functional form of the M–O similarity functions in the surface layer. The similarity functions predicted for the stable-continuous regime are in good agreement with available empirical data for the steady and the evolving-with-time ABL.

In the convective case, locally scaled similarity functions are postulated to be constant (except Φ_M) in the lower half of the mixed layer. It has been shown that functions Φ_h, Φ_w, Φ_θ, $\Phi_{1\theta}$, $\Phi_{3\theta}$, Φ_{w3} obey local similarity. Although the function Φ_M behaves as predicted, it does not follow the local similarity.

Acknowledgements

The author would like to express his gratitude to Prof. R. A. Brown, Prof. J. M. Wallace (Chairman of the Department) and Prof. J. A. Businger, for making his visit possible in the Department of Atmospheric Sciences, University of Washington, Seattle, where this paper has been completed. In addition, I want to thank Mrs. Sylvia Lavin for helping with the preparation of this manuscript.

References

Arya, S. P. S.: 1982, 'Atmospheric Boundary Layers over Homogeneous Terrain', in *Engineering Meteorology*, E. J. Plate (ed.), Elsevier Scientific Publ. Co., 233–268.

Businger, J. A., Wyngaard, J. C., Izumi, Y., and Bradley, E. F.: 1971, 'Fluxprofile Relationship in the Atmospheric Surface Layer', *J. Atmos. Sci.* **78**, 181–189.

Caughey, S. J. and Readings, C. J.: 1974, 'The Vertical Component of Turbulence in Convective Conditions', *Advances in Geophys.* **18A**, 125–130.

Caughey, S. J. and Readings, C. J.: 1975, 'Turbulent Fluctuations in Convective Conditions', *Quart. J. Roy. Meteorol. Soc.* **101**, 537–542.

Caughey, S. J. and Palmer, S. G.: 1979, 'Some Aspects of Turbulence Structure Through the Depth of the Convective Boundary Layer', *Quart. J. Roy. Meteorol. Soc.* **105**, 811–827.

Caughey, S. J., Wyngaard, J. C., and Kaimal, J. C.: 1979, 'Turbulence in the Evolving Stable Boundary Layer', *J. Atmos. Sci.* **36**, 1041–1052.

Deardorff, J. W.: 1970, 'Convective Velocity and Temperature Scales for the Unstable Planetary Boundary Layer and Temperature Scales for the Unstable Planetary Boundary Layer and for Rayleigh Convection', *J. Atmos. Sci.* **27**, 1211–1213.

Deardorff, J. W.: 1978, 'Observed Characteristics of the Outer Layer', AMS course on the Planetary Boundary Layer. Boulder, CO (unpublished manuscript).

Izumi, Y. and Caughey, J. S.: 1976, *Minnesota 1973 Atmospheric Boundary Layer Experiment Data Report*, Air Force Cambridge Research Laboratories. AFCRL-TR-76-0038. Environmental Research Papers, No. 547.

Kaimal, J. C., Wyngaard, J. C., Haugen, D. A., Coté, O. R., Izumi, Y., Caughey, J. C., and Readings, C. J.: 1976, 'Turbulence Structure in the Convective Boundary Layer', *J. Atmos. Sci.* **33**, 2152–2169.

Lenschow, D. H., Wyngaard, J. C., and Pennell, W. T.: 1980, 'Mean-Field and Second-Moment Budgets in a Baroclinic Convective Boundary Layer', *J. Atmos. Sci.* **37**, 1313–1326.

Lilly, D. K.: 1968, 'Models of Cloud-Topped Mixed Layers Under a Strong Inversion', *Quart. J. Roy. Meteorol. Soc.* **94**, 292–309.

Monin, A. S. and Obukhov, A. M.: 1954, 'Basic Laws of Turbulent Mixing in the Atmosphere near the Ground', Tr. Akad Nauk, SSSR Geophiz. Inst., No. 24 (151), 1963–1987.

Nieuwstadt, F. T. M.: 1984, 'The Turbulent Structure of the Stable, Nocturnal Boundary Layer', *J. Atmos. Sci.* **41**, 2202–2216.

Takeuchi, K.: 1961, 'On the Structure of the Turbulent Field in the Surface Boundary Layer', *J. Meteorol. Soc. Japan*, Set II, **39**, 6, 346–364.

Tennekes, H. and Lumley, J. L.: 1972, *A First Course in Turbulence*, MIT Press, Boston, MA.

Wyngaard, J. C., Coté, O. R., and Izumi, Y.: 1971, 'Local Free Convection, Similarity and Budgets of Shear Stress and Heat Flux'. *J. Atmos. Sci.* **28**, 1171–1182.

Wyngaard, J. C.: 1973, 'On Surface Layer Turbulence', in D. A. Haugen (ed.), *Workshop on Micrometeorology*, American Meteorological Soc., pp. 101–148.

Yokoyama, O., Gamo, M., and Yamamoto, S.: 1979, 'The Vertical Profiles of the Turbulence Quantities in the Atmospheric Boundary Layer', *J. Meteorol. Soc. Japan* **57**, 3, 264–272.

Zilitinkevich, S. S. and Chalikov, D. V.: 1968, 'On the Determination of the Universal Wind and Temperature Profiles in the Surface Layer of the Atmosphere', *Izv. Akad. Nauk SSSR, Fiz. Atm. i Okeana (Bull. Acad. Sci., USSR, Atmospheric and Oceanic Physics)* **4**, 294–302.